Helfrich Brownian Dynamics in Linear Monge Gauge

Samuel Foley

March 2025

Abstract

The Brownian equations of motion for the small-gradient approximation of the Helfrich energy are derived. We begin from first principles via low Reynolds number hydrodynamics (Stokes equations) applied to colloid particle suspensions and then adapt the result to fluid membranes. This treatment very closely follows the presentation in chapter 3 of Doi and Edwards's *The Theory of Polymer Dynamics* [3] in order to derive the methods of Lin and Brown's 2004 *Phys. Rev. Lett.* [4]. For alternative derivations and related models, see [1] and [5].

1 Hydrodynamic Interactions Between Colloid Particles

1.1 Governing Equations

Suppose N point-like Brownian particles which move with their surrounding fluid have locations $\mathbf{R}_n$ and are each subject to an external force $\mathbf{F}_n$. These applied forces and resulting particle motion induce motion in the surrounding fluid which couples all of their dynamics. We seek an expression for the velocity field $\mathbf{v}(\mathbf{r})$ of the fluid in terms of the forces and positions. We do this under the assumptions of fluid incompressibility

$$\nabla \cdot \mathbf{v} = 0 \tag{1}$$

and negligible fluid inertia, which means ignoring the $\mathrm{D}\mathbf{v}/\mathrm{D}t$ term in the Navier-Stokes equations, leaving us with

$$\nabla \cdot \boldsymbol{\sigma} + \mathbf{f} = 0, \tag{2}$$

where $\boldsymbol{\sigma}$ is the local stress tensor and $\mathbf{f}$ is the local external force per unit volume. In words, this says that the fluid is always in local mechanical equilibrium; any forces $\mathbf{f}$ applied are immediately balanced by the internal fluid stress $\boldsymbol{\sigma}$. The usual constitutive equation for an incompressible Newtonian fluid relates stress to strain-rate in the form

$$\boldsymbol{\sigma} = \eta\left(\nabla\mathbf{v} + (\nabla\mathbf{v})^\top\right) - P\mathbb{I}, \tag{3}$$

in which η is the (dynamic) viscosity and P the bulk pressure. The quantity $\boldsymbol{\varepsilon} = (\nabla\mathbf{v}+(\nabla\mathbf{v})^\top)/2$ is known as the strain-rate tensor, which allows eqn. (3) to be written much more compactly as $\boldsymbol{\sigma} = 2\eta\boldsymbol{\varepsilon} - P\mathbb{I}$. Taking the divergence of eqn. (3) gives

$$\nabla \cdot \boldsymbol{\sigma} = \eta\nabla^2\mathbf{v} + \eta\nabla\cdot(\nabla\mathbf{v})^\top - \nabla P.$$

The second term is zero due to eqn. (1), which is easiest seen in component form:

$$\left(\nabla\cdot(\nabla\mathbf{v})^\top\right)_\alpha = \partial_\beta\partial_\alpha v_\beta = \partial_\alpha\partial_\beta v_\beta = \big(\nabla(\underbrace{\nabla\cdot\mathbf{v}}_{=0})\big)_\alpha = 0.$$

Combined with eqn. (2), this brings us to

$$\boxed{\eta\nabla^2\mathbf{v} - \nabla P + \mathbf{f} = 0} \tag{4}$$

Equations (1) and (4) together are known as the Stokes equations of motion for an incompressible Newtonian fluid. Our goal is now to solve this PDE for the velocity field $\mathbf{v}$, given some $\mathbf{f}$. We can then also compute the resulting pressure field P if so desired (up to an additive constant, since P only enters as ∇P).

1.2 Solution via Fourier Transform

We define our 3-dimensional Fourier Transform as

$$\tilde{f}(\mathbf{k}) = \int \mathrm{d}V\, f(\mathbf{r}) e^{-i\mathbf{k}\cdot\mathbf{r}}.$$

Applying this to eqns. (1) and (4) we get

$$i\mathbf{k}\cdot\tilde{\mathbf{v}} = 0, \tag{5}$$

$$-\eta k^2 \tilde{\mathbf{v}} - i\mathbf{k}\tilde{P} + \tilde{\mathbf{f}} = 0. \tag{6}$$

Rearranging the last equation, we have

$$\tilde{\mathbf{v}} = \frac{1}{\eta k^2}\left(\tilde{\mathbf{f}} - i\mathbf{k}\tilde{P}\right).$$

Equation (5) tells us that $\tilde{\mathbf{v}}(\mathbf{k})$ is orthogonal to $\mathbf{k}$, so it must be that $\tilde{\mathbf{f}}$ cancels the pressure contribution. To show this explicitly, we dot the above with $\mathbf{k}$ and find

$$\begin{aligned}
\tilde{\mathbf{v}}\cdot\mathbf{k} &= \frac{1}{\eta k^2}\left(\tilde{\mathbf{f}}\cdot\mathbf{k} - ik^2\tilde{P}\right)\\
&= \frac{1}{\eta k}\tilde{\mathbf{f}}\cdot\hat{\mathbf{k}} - \frac{i}{\eta}\tilde{P} = 0\\
\implies \tilde{P} &= \frac{1}{ik}\hat{\mathbf{k}}\cdot\tilde{\mathbf{f}}
\end{aligned}$$

Plugging this back into our equation for $\tilde{\mathbf{v}}$ gives

$$\tilde{\mathbf{v}} = \frac{1}{\eta k^2}\left(\tilde{\mathbf{f}} - i\mathbf{k}\left(\frac{1}{ik}\hat{\mathbf{k}}\cdot\tilde{\mathbf{f}}\right)\right) = \frac{1}{\eta k^2}\left(\tilde{\mathbf{f}} - \hat{\mathbf{k}}(\hat{\mathbf{k}}\cdot\tilde{\mathbf{f}})\right),$$

and so we find the neat result

$$\tilde{\mathbf{v}} = \frac{1}{\eta k^2}\left(\mathbb{I} - \hat{\mathbf{k}}\hat{\mathbf{k}}^\top\right)\tilde{\mathbf{f}}. \tag{7}$$

We must now invert the Fourier transform to get our real-space result $\mathbf{v}(\mathbf{r})$,

$$\begin{aligned}
\mathbf{v}(\mathbf{r}) &= \frac{1}{(2\pi)^3}\int \mathrm{d}^3k\, \tilde{\mathbf{v}}(\mathbf{k})e^{i\mathbf{k}\cdot\mathbf{r}}\\
&= \frac{1}{8\pi^3\eta}\int \mathrm{d}^3k\, \frac{1}{k^2}\left(\mathbb{I} - \hat{\mathbf{k}}\hat{\mathbf{k}}^\top\right)\tilde{\mathbf{f}}(\mathbf{k})e^{i\mathbf{k}\cdot\mathbf{r}}\\
&= \frac{1}{8\pi^3\eta}\int \mathrm{d}^3k\, \frac{1}{k^2}\left(\mathbb{I} - \hat{\mathbf{k}}\hat{\mathbf{k}}^\top\right)\left(\int \mathrm{d}V'\mathbf{f}(\mathbf{r}')e^{-i\mathbf{k}\cdot\mathbf{r}'}\right)e^{i\mathbf{k}\cdot\mathbf{r}}\\
&= \frac{1}{8\pi^3\eta}\int \mathrm{d}V'\int \mathrm{d}^3k\, \frac{1}{k^2}\left(\mathbb{I} - \hat{\mathbf{k}}\hat{\mathbf{k}}^\top\right)e^{i\mathbf{k}\cdot(\mathbf{r}-\mathbf{r}')}\mathbf{f}(\mathbf{r}')\\
&\boxed{\mathbf{v}(\mathbf{r}) = \int \mathsf{H}(\mathbf{r}-\mathbf{r}')\mathbf{f}(\mathbf{r}')\mathrm{d}V'}
\end{aligned} \tag{8}$$

wherein the last line we have implicitly defined the Fourier representation of the **Oseen Tensor** H:

$$\mathsf{H}(\mathbf{r}) = \frac{1}{8\pi^3\eta}\int \mathrm{d}^3k\, \frac{1}{k^2}\left(\mathbb{I} - \hat{\mathbf{k}}\hat{\mathbf{k}}^\top\right)e^{i\mathbf{k}\cdot\mathbf{r}}, \tag{9}$$

which is the Green's function for the velocity field of Stokes flow in an unbounded domain.

1.3 The Oseen Tensor

The evaluation of eqn. (9) is made less painful by recognizing that the form of $\mathsf{H}(\mathbf{r})$ is restricted by symmetries (see aside box). Rather than trying to attack eqn. (9) head-on, we can try to figure out $a(r)$ and $b(r)$ in eqn. (10) by looking at two scalars that we can calculate from both representations of H.

The trace of H is, according to eqn. (10),

$$\mathrm{Tr}(\mathsf{H}) = h_{\alpha\alpha} = 3a(r) + b(r). \tag{11}$$

Aside: Symmetries Restrict the Form of H

The Oseen tensor $\mathsf{H} = \mathsf{H}(\mathbf{r})$ depends only on $\mathbf{r}$, and as a geometric object knows about nothing else. Without loss of generality, let us define our (Cartesian) coordinate system such that $\hat{\mathbf{r}} = \hat{\mathbf{z}}$. Each component of H is $h_{ij} = h_{ij}(r)$ since $\mathbf{r} = r\hat{\mathbf{z}}$. The complete matrix representation is

$$\mathsf{H} = \begin{pmatrix} h_{11} & h_{12} & h_{13} \\ h_{21} & h_{22} & h_{23} \\ h_{31} & h_{32} & h_{33} \end{pmatrix}.$$

The matrix must be identical in bases which are related via operations that leave $\mathbf{r}$ unchanged (symmetries).
Rotate by $\pi/2$ about $\hat{\mathbf{z}}$:

$$\mathsf{H} = \mathsf{R}_{\frac{\pi}{2}} \mathsf{H} \mathsf{R}_{\frac{\pi}{2}}^{-1} \quad \leftrightarrow \quad \begin{pmatrix} h_{11} & h_{12} & h_{13} \\ h_{21} & h_{22} & h_{23} \\ h_{31} & h_{32} & h_{33} \end{pmatrix} = \begin{pmatrix} h_{22} & -h_{21} & -h_{23} \\ -h_{12} & h_{11} & h_{13} \\ -h_{32} & h_{31} & h_{33} \end{pmatrix}$$

$$\implies h_{13} = h_{23} = h_{31} = h_{32} = 0, \quad h_{12} = -h_{21}, \quad h_{22} = h_{11}$$

$$\implies \mathsf{H} = \begin{pmatrix} h_{11} & h_{12} & 0 \\ -h_{12} & h_{11} & 0 \\ 0 & 0 & h_{33} \end{pmatrix}$$

Reflect $x \to -x$:

$$\mathsf{H} = \mathsf{R}_{-x} \mathsf{H} \mathsf{R}_{-x} \quad \leftrightarrow \quad \begin{pmatrix} h_{11} & h_{12} & 0 \\ -h_{12} & h_{11} & 0 \\ 0 & 0 & h_{33} \end{pmatrix} = \begin{pmatrix} h_{11} & -h_{12} & 0 \\ h_{12} & h_{11} & 0 \\ 0 & 0 & h_{33} \end{pmatrix}$$

$$\implies h_{12} = 0$$

So,

$$\mathsf{H} = \begin{pmatrix} h_{11} & 0 & 0 \\ 0 & h_{11} & 0 \\ 0 & 0 & h_{33} \end{pmatrix} = \begin{pmatrix} a & 0 & 0 \\ 0 & a & 0 \\ 0 & 0 & a+b \end{pmatrix} = a\mathbb{I} + b\hat{\mathbf{z}}\hat{\mathbf{z}}^\top$$

$$\boxed{\mathsf{H}(\mathbf{r}) = a(r)\mathbb{I} + b(r)\hat{\mathbf{r}}\hat{\mathbf{r}}^\top} \tag{10}$$

We can also calculate the trace as

$$\begin{aligned} \mathrm{Tr}(\mathsf{H}) &= \mathrm{Tr}\left(\frac{1}{8\pi^3\eta}\int \mathrm{d}^3k\,\frac{1}{k^2}\left(\mathbb{I} - \hat{\mathbf{k}}\hat{\mathbf{k}}^\top\right)e^{i\mathbf{k}\cdot\mathbf{r}}\right) \\ &= \frac{1}{8\pi^3\eta}\int \mathrm{d}^3k\,\frac{1}{k^2}\Big[\underbrace{\mathrm{Tr}\left(\mathbb{I}\right)}_{3} - \underbrace{\mathrm{Tr}\left(\hat{\mathbf{k}}\hat{\mathbf{k}}^\top\right)}_{1}\Big]e^{i\mathbf{k}\cdot\mathbf{r}} \\ &= \frac{1}{8\pi^3\eta}\int \mathrm{d}^3k\,\frac{2}{k^2}e^{i\mathbf{k}\cdot\mathbf{r}} \end{aligned}$$

At this point we can try to look up the result in a table of Fourier transforms or be brave and compute the integral in spherical $\mathbf{k}$ coordinates with the polar axis along $\hat{\mathbf{r}}$. Thus $\mathrm{d}^3k = k^2 \sin\theta\,\mathrm{d}k\,\mathrm{d}\theta\,\mathrm{d}\phi$ and we have

$$\begin{aligned} \mathrm{Tr}(\mathsf{H}) = \frac{1}{4\pi^3\eta}\int_0^\infty \mathrm{d}k \int_0^\pi \mathrm{d}\theta \int_0^{2\pi} \mathrm{d}\phi \sin\theta e^{ikr\cos\theta} &= \frac{1}{2\pi^2\eta}\int_0^\infty \mathrm{d}k \int_0^\pi \mathrm{d}\theta \sin\theta e^{ikr\cos\theta} \\ &= \frac{1}{2\pi^2\eta}\int_0^\infty \mathrm{d}k \int_{-1}^1 \mathrm{d}u\, e^{ikru} \end{aligned}$$

$$= \frac{1}{2\pi^2\eta}\int_0^\infty \mathrm{d}k \frac{1}{ikr}\left(e^{ikr} - e^{-ikr}\right) = \frac{1}{\pi^2\eta}\int_0^\infty \mathrm{d}k \frac{\sin(kr)}{kr} = \frac{1}{2\pi\eta r}.$$

For our second scalar, we will take $\hat{\mathbf{r}}^\top \mathsf{H}\,\hat{\mathbf{r}} = a(r) + b(r)$. In terms of eqn. (9), this is

$$\hat{\mathbf{r}}^\top \mathsf{H}\,\hat{\mathbf{r}} = \frac{1}{8\pi^3\eta}\int \mathrm{d}^3k\,\frac{1}{k^2}\left(\hat{\mathbf{r}}^\top\hat{\mathbf{r}} - \hat{\mathbf{r}}^\top\hat{\mathbf{k}}\hat{\mathbf{k}}^\top\hat{\mathbf{r}}\right)e^{i\mathbf{k}\cdot\mathbf{r}} = \frac{1}{8\pi^3\eta}\int \mathrm{d}^3k\,\frac{1}{k^2}\left(1 - \left(\hat{\mathbf{k}}\cdot\hat{\mathbf{r}}\right)^2\right)e^{i\mathbf{k}\cdot\mathbf{r}}.$$

Once again changing to spherical coordinates,

$$\hat{\mathbf{r}}^\top \mathsf{H}\,\hat{\mathbf{r}} = \frac{2\pi}{8\pi^3\eta}\int_0^\infty \mathrm{d}k \int_0^\pi \mathrm{d}\theta \sin\theta\left(1 - \cos^2\theta\right)e^{ikr\cos\theta} = \frac{1}{4\pi^2\eta}\int_0^\infty \mathrm{d}k\int_{-1}^1 \mathrm{d}u\left(1 - u^2\right)e^{ikru}.$$

The first term is the same as one of the integrals we computed above, and the second term integrates to zero after some (read: much) tedium. So, the result is

$$\hat{\mathbf{r}}^\top \mathsf{H}\,\hat{\mathbf{r}} = \frac{1}{4\pi\eta r}.$$

Thus we have

$$3a + b = \frac{1}{2\pi\eta r} \quad \text{and} \quad a + b = \frac{1}{4\pi\eta r}$$
$$\Longrightarrow\ a(r) = b(r) = \frac{1}{8\pi\eta r},$$

and together with eqn. (10), we can finally write down the Oseen Tensor in real space.

$$\boxed{\mathsf{H}(\mathbf{r}) = \frac{1}{8\pi\eta r}\left(\mathbb{I} + \hat{\mathbf{r}}\hat{\mathbf{r}}^\top\right)} \tag{12}$$

1.4 Putting it All Together

For forces applied to point particles located at $\mathbf{R}_n$, the external force density $\mathbf{f}$ is

$$\mathbf{f}(\mathbf{r}) = \sum_{n=1}^N \mathbf{F}_n\delta^3(\mathbf{r} - \mathbf{R}_n). \tag{13}$$

By inserting this into eqn. (8), we get the nicely compact solution:

$$\mathbf{v}(\mathbf{r}) = \int \mathsf{H}(\mathbf{r} - \mathbf{r}')\sum_{n=1}^N \mathbf{F}_n\delta^3(\mathbf{r}' - \mathbf{R}_n)\mathrm{d}V' = \sum_{n=1}^N \mathsf{H}(\mathbf{r} - \mathbf{R}_n)\mathbf{F}_n. \tag{14}$$

There is still one outstanding issue: $\mathbf{v}(\mathbf{r})$ diverges whenever $\mathbf{r} \to \mathbf{R}_n$. This arises out of our choosing to model our particles as infinitesimal points rather than spheres of finite radius. This is rather unfortunate though, since the velocities of the colloid particles located at $\mathbf{r} = \mathbf{R}_n$ are the main point of interest here. To avoid this, Doi and Edwards suggest an approximation based on Stokes's Law. The steady velocity of an *isolated* spherical particle of finite radius a subject to a force $\mathbf{F}$ (or, equivalently, the viscous drag force on a stationary sphere immersed in a far-field flow $\mathbf{v}$) can actually be solved exactly from eqns. (1) and (4), the result being

$$\mathbf{v} = \frac{\mathbf{F}}{6\pi\eta a} = \frac{\mathbb{I}}{\zeta}\mathbf{F}, \tag{15}$$

defining $\zeta = 6\pi\eta a$. This result is known as Stokes's Law. Based on this, it is suggested that when calculating the velocity $\mathbf{V}_m$ of a particle located at $\mathbf{R}_m$,

$$\mathbf{V}_m = \sum_{n=1}^N \mathsf{H}(\mathbf{R}_m - \mathbf{R}_n)\mathbf{F}_n, \tag{16}$$

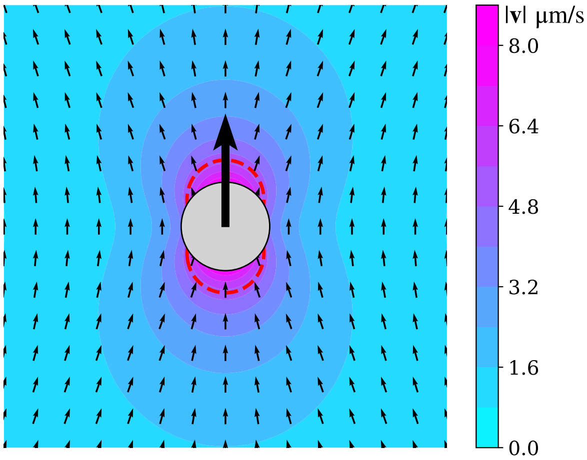

Figure 1: Plot of the velocity field $\mathbf{v}(\mathbf{r})$ around a particle subject to a force $\mathbf{F} = (1\,\mathrm{pN})\hat{\mathbf{y}}$ as calculated from eqn. (14). Arrows depict $\hat{\mathbf{v}}$, color indicates speed $v = |\mathbf{v}|$. The dashed red curve indicates the contour $v = F/6\pi\eta a$, the particle speed predicted from Stokes's Law. The outermost extent of this contour may serve as a reasonable cutoff beyond which the point-particle approximation can be trusted. Particle radius $a = 100\,\mathrm{nm}$ and the plotted region measures $1\mathrm{\mu m} \times 1\mathrm{\mu m}$. The viscosity $\eta = 6$ centipoise, roughly the viscosity of cytosol (a bit more viscous than pure water ≈ 1 cP).

one can replace the divergent $\mathsf{H}(0)$ in the $n = m$ term by $\mathbb{I}/\zeta$ as a reasonable approximation. This can then be seen as a lowest-order correction to Stokes's law accounting for the presence of other particles, by treating them as point-like.

Figure 1 shows a plot of the velocity field $\mathbf{v}(\mathbf{r})$ around a single particle subject to a force in the positive $\hat{\mathbf{y}}$ direction as calculated from our point-particle solution eqn. (14). To get an idea for what distance can be considered "far enough" away from the particle for the point approximation to be acceptable, Fig. 1 also plots a dashed red curve indicating the locations at which the magnitude of $\mathbf{v}(\mathbf{r})$ is equal to the speed from Stokes's law, eqn. (15), which can be solved in closed form in polar coordinates,

$$\begin{aligned} \left| \frac{1}{8\pi\eta r} \left(\mathbb{I} + \hat{\mathbf{r}}\hat{\mathbf{r}}^\top \right) F\hat{\mathbf{y}} \right| &= \frac{F}{6\pi\eta a} \\ \frac{1}{4r} \left| \sin\theta\cos\theta\,\hat{\mathbf{x}} + (1+\sin^2\theta)\hat{\mathbf{y}} \right| &= \frac{1}{3a} \\ \implies r(\theta) &= \frac{3}{4} a \sqrt{\sin^2\theta\cos^2\theta + (1+\sin^2\theta)^2}. \end{aligned}$$

This depends only on the particle radius a, and has maxima of $r = 3a/2$ at $\theta = \pm\pi/2$, suggesting that we might trust the result for $r > 3a/2$.

2 Small-Gradient Helfrich Dynamics

2.1 Real Space

The Helfrich energy functional for a membrane (represented as a 2-dimensional surface $\mathcal{M}$) with no spontaneous curvature and constant tension σ is[1]

$$E^*[\mathcal{M}] = \int_{\mathcal{M}} \mathrm{d}A \left\{ \frac{1}{2}\kappa K^2 + \bar{\kappa} K_\mathrm{G} + \sigma \right\}. \tag{17}$$

κ and $\bar{\kappa}$ are the curvature and Gaussian moduli, respectively, and they predictably multiply the curvature K and Gaussian curvature K_G. We will assume that the membrane has no boundary and undergoes no topological changes; therefore we can discard the integral of K_G since it does not change due to the Gauss-Bonnet theorem. We will also confine our interest to membranes which are nearly flat, such that

[1] I apologize for re-using the letter σ. Bold $\boldsymbol{\sigma}$ was the stress tensor above, normal σ here will be membrane tension.

$|\nabla h| \ll 1$, with $h(x,y)$ being the height function describing our membrane shape (the so-called Monge gauge). In this case, $\mathrm{d}A = \mathrm{d}x\mathrm{d}y\sqrt{1+(\nabla h)^2} \approx \mathrm{d}x\mathrm{d}y(1+\frac{1}{2}(\nabla h)^2)$ and $K \approx \nabla^2 h$. Discarding a constant term we are left with the lowest order approximation

$$E^*[\mathcal{M}] \approx E[h] = \int_{\mathbb{R}^2} \mathrm{d}x\mathrm{d}y \left\{ \frac{1}{2}\kappa(\nabla^2 h)^2 + \frac{1}{2}\sigma(\nabla h)^2 \right\}. \tag{18}$$

The local force per unit area in the $\hat{\mathbf{z}}$ direction (since we only allow the $\hat{\mathbf{z}}$ degree of freedom h to vary) for a given shape $h(x,y)$ is given by the functional derivative of this energy,[2]

$$\mathcal{F}(x,y) = -\frac{\delta E}{\delta h}(x,y) = \sigma\nabla^2 h - \kappa\nabla^4 h. \tag{19}$$

In accordance with the small gradient approximation, we consider the net tangential forces to be negligible. With no other forces acting, we can write the force per unit volume in the entire medium as

$$\mathbf{f}(\mathbf{r}) = \mathcal{F}(x,y)\delta(z-h(x,y))\hat{\mathbf{z}}. \tag{20}$$

Once again, we are considering membranes which are very nearly flat, so we will further approximate this as $\mathbf{f}(\mathbf{r}) \approx \mathcal{F}(x,y)\delta(z)$ to simplify our next calculation. In the following, I will use $\mathbf{r}$ to denote a 3-dimensional position vector and $\boldsymbol{\rho}$ to denote a position vector restricted to the xy-plane. Appealing to eqn. (8), we can say that the local membrane velocity in the $\hat{\mathbf{z}}$ direction is

$$\begin{aligned}
\partial_t h(\boldsymbol{\rho}) = \hat{\mathbf{z}}\cdot\mathbf{v}(\boldsymbol{\rho}+h(\boldsymbol{\rho})\hat{\mathbf{z}}) \approx \hat{\mathbf{z}}\cdot\mathbf{v}(\boldsymbol{\rho}) &= \hat{\mathbf{z}}\cdot\int \mathsf{H}(\boldsymbol{\rho}-\mathbf{r}')\mathbf{f}(\mathbf{r}')\,\mathrm{d}x'\mathrm{d}y'\mathrm{d}z' \\
&\approx \hat{\mathbf{z}}\cdot\int \mathsf{H}(\boldsymbol{\rho}-\mathbf{r}')\mathcal{F}(x',y')\delta(z')\hat{\mathbf{z}}\,\mathrm{d}x'\mathrm{d}y'\mathrm{d}z' \\
&= \hat{\mathbf{z}}\cdot\int \mathsf{H}(\boldsymbol{\rho}-\boldsymbol{\rho}')\mathcal{F}(x',y')\hat{\mathbf{z}}\,\mathrm{d}x'\mathrm{d}y' \\
&= \hat{\mathbf{z}}\cdot\int \frac{1}{8\pi\eta|\boldsymbol{\rho}-\boldsymbol{\rho}'|}\left(\hat{\mathbf{z}} + \frac{(\boldsymbol{\rho}-\boldsymbol{\rho}')(\boldsymbol{\rho}-\boldsymbol{\rho}')\cdot\hat{\mathbf{z}}}{|\boldsymbol{\rho}-\boldsymbol{\rho}'|^2}\right)\mathcal{F}(x',y')\,\mathrm{d}x'\mathrm{d}y'.
\end{aligned}$$

Since $(\boldsymbol{\rho}-\boldsymbol{\rho}')\cdot\hat{\mathbf{z}} = 0$, we immediately have

$$\boxed{\partial_t h(\boldsymbol{\rho}) = \int_{\mathbb{R}^2} \frac{1}{8\pi\eta|\boldsymbol{\rho}-\boldsymbol{\rho}'|}\mathcal{F}(\boldsymbol{\rho}')\mathrm{d}x'\mathrm{d}y'} \tag{21}$$

Thus, the non-local hydrodynamic interactions couple the motion of each point to the force on all other points on the membrane (instantaneously, in the Stokes approximation).

2.2 Fourier Space

Having to calculate an integral over the entire membrane for every point we propagate forward in time is less than ideal. Looking back at eqn. (7), we can see that in Fourier space, $\tilde{\mathbf{v}}(\mathbf{k})$ can be calculated from $\tilde{\mathbf{f}}(\mathbf{k})$ without a convolution over all $\mathbf{k}$ modes. Of course, that's assuming we already know the Fourier transform of the forces. Let's derive the equivalent expression for our membrane equation of motion.

From this point onward, we will restrict our consideration to a finite square patch of membrane over a domain with side length L. This is for two main reasons: (1) the statistical mechanics of continuous fields is a very tricky business which is made conceptually simpler by periodicity, as it allows us to work with a discrete basis of Fourier modes $\mathbf{k} = \frac{2\pi}{L}(n\hat{\mathbf{x}} + m\hat{\mathbf{y}})$ and (2) the ulterior motive this whole time has been to derive a membrane simulation algorithm which will necessarily be applied to systems with finite size (and resolution). With this in mind, we write our height and normal force per unit area as Fourier series,

$$h(\mathbf{r},t) = \frac{1}{L}\sum_{\mathbf{k}} h_{\mathbf{k}}(t)e^{i\mathbf{k}\cdot\mathbf{r}}, \qquad \mathcal{F}(\mathbf{r},t) = \frac{1}{L}\sum_{\mathbf{k}} \mathcal{F}_{\mathbf{k}}(t)e^{i\mathbf{k}\cdot\mathbf{r}}. \tag{22}$$

[2]If one wants *all* the membrane force components for an arbitrary shape, they can be found by calculating the divergence of the membrane stress tensor, requiring a much more involved functional variation procedure, see [2].

Plugging these expressions into eqn. (21) and simplifying, we find

$$\begin{aligned}
\dot{h}(\mathbf{r},t) &= \frac{1}{8\pi\eta}\int\limits_{\mathbb{R}^2}\frac{\mathrm{d}x'\mathrm{d}y'}{|\mathbf{r}-\mathbf{r}'|}\left[\frac{1}{L}\sum_{\mathbf{k}}\mathcal{F}_{\mathbf{k}}(t)e^{i\mathbf{k}\cdot\mathbf{r}'}\right] \\
&= \frac{1}{8\pi\eta L}\sum_{\mathbf{k}}\mathcal{F}_{\mathbf{k}}(t)\int\limits_{\mathbb{R}^2}\frac{\mathrm{d}x'\mathrm{d}y'}{|\mathbf{r}-\mathbf{r}'|}e^{i\mathbf{k}\cdot\mathbf{r}'} \\
&= \frac{1}{8\pi\eta L}\sum_{\mathbf{k}}\mathcal{F}_{\mathbf{k}}(t)\int\limits_{\mathbb{R}^2}\frac{\mathrm{d}x''\mathrm{d}y''}{|\mathbf{r}''|}e^{i\mathbf{k}\cdot(\mathbf{r}-\mathbf{r}'')} \\
&= \frac{1}{8\pi\eta L}\sum_{\mathbf{k}}\mathcal{F}_{\mathbf{k}}(t)e^{i\mathbf{k}\cdot\mathbf{r}}\int\limits_{\mathbb{R}^2}\frac{\mathrm{d}x''\mathrm{d}y''}{|\mathbf{r}''|}e^{-i\mathbf{k}\cdot\mathbf{r}''} \\
&= \frac{1}{L}\sum_{\mathbf{k}}\mathcal{F}_{\mathbf{k}}(t)e^{i\mathbf{k}\cdot\mathbf{r}}\frac{1}{8\pi\eta}\int\limits_{\mathbb{R}^2}\frac{\mathrm{d}x''\mathrm{d}y''}{|\mathbf{r}''|}e^{-i\mathbf{k}\cdot\mathbf{r}''} \\
\frac{1}{L}\sum_{\mathbf{k}}\dot{h}_{\mathbf{k}}(t)e^{i\mathbf{k}\cdot\mathbf{r}} &= \frac{1}{L}\sum_{\mathbf{k}}\Lambda_{\mathbf{k}}\mathcal{F}_{\mathbf{k}}(t)e^{i\mathbf{k}\cdot\mathbf{r}} \\
&\implies \boxed{\dot{h}_{\mathbf{k}} = \Lambda_{\mathbf{k}}\mathcal{F}_{\mathbf{k}}}
\end{aligned} \tag{23}$$

Where we have once again defined an Oseen parameter,

$$\Lambda_{\mathbf{k}} = \frac{1}{8\pi\eta}\int\limits_{\mathbb{R}^2}\frac{\mathrm{d}x\mathrm{d}y}{r}e^{-i\mathbf{k}\cdot\mathbf{r}} = \frac{1}{8\pi\eta}\int\limits_0^{2\pi}\mathrm{d}\theta\int\limits_0^{\infty}\mathrm{d}r\, e^{-ikr\cos\theta} \overset{*}{=} \frac{2\pi}{8\pi\eta}\int\limits_0^{\infty}J_0(kr)\mathrm{d}r = \frac{1}{4\eta k}.$$

At the * we made use of an integral representation of the $n=0$ Bessel function of the first kind [6],

$$J_0(z) = \frac{1}{2\pi}\int\limits_0^{2\pi}e^{iz\cos\theta}\mathrm{d}\theta.$$

The equations of motion in Fourier space are beautifully simple, but it gets even better when we write the membrane forces in eqn. (19) in Fourier representation. For this we need the Laplacian and bi-Laplacian of the membrane height, which are easy to compute in Fourier space:

$$\begin{aligned}
\nabla h(\mathbf{r},t) &= \frac{1}{L}\sum_{\mathbf{k}}ih_{\mathbf{k}}(t)\mathbf{k}e^{i\mathbf{k}\cdot\mathbf{r}} & \nabla^2 h(\mathbf{r},t) &= -\frac{1}{L}\sum_{\mathbf{k}}k^2h_{\mathbf{k}}(t)e^{i\mathbf{k}\cdot\mathbf{r}} \\
\nabla^3 h(\mathbf{r},t) &= -\frac{1}{L}\sum_{\mathbf{k}}ik^2h_{\mathbf{k}}(t)\mathbf{k}e^{i\mathbf{k}\cdot\mathbf{r}} & \nabla^4 h(\mathbf{r},t) &= \frac{1}{L}\sum_{\mathbf{k}}k^4h_{\mathbf{k}}(t)e^{i\mathbf{k}\cdot\mathbf{r}}
\end{aligned}$$

Thus, we have

$$\begin{aligned}
\mathcal{F}(\mathbf{r},t) = \sigma\nabla^2 h - \kappa\nabla^4 h = -\frac{1}{L}\sum_{\mathbf{k}}\left(\kappa k^4+\sigma k^2\right)h_{\mathbf{k}}(t)e^{i\mathbf{k}\cdot\mathbf{r}} &= \frac{1}{L}\sum_{\mathbf{k}}\mathcal{F}_{\mathbf{k}}(t)e^{i\mathbf{k}\cdot\mathbf{r}} \\
\implies \boxed{\mathcal{F}_{\mathbf{k}} = -(\kappa k^4+\sigma k^2)h_{\mathbf{k}}}
\end{aligned} \tag{24}$$

Our equation of motion $\dot{h}_{\mathbf{k}}(t) = -\Lambda_{\mathbf{k}}(\kappa k^4+\sigma k^2)h_{\mathbf{k}}(t)$ is thus a simple first-order linear system, so the relaxation in response to an instantaneous perturbation at time $t=0$ is exponential,

$$h_{\mathbf{k}}^{\mathrm{GF}}(t) = e^{-\Lambda_{\mathbf{k}}(\kappa k^4+\sigma k^2)t}\Theta(t). \tag{25}$$

This is the temporal Green's function, and from it we can immediately read off the characteristic relaxation time $\tau_k = 1/\Lambda_k(\kappa k^4+\sigma k^2)$ for a given membrane undulation mode:

$$\boxed{\tau_k = \frac{4\eta}{\kappa k^3+\sigma k}} \tag{26}$$

2.3 Stochastic Dynamics: Fluctuation-Dissipation Theorem

So far, all of the equations have been fully deterministic. This may be reasonable for simulations on sufficiently large length scales (provided one is still in the small Reynolds number regime), but for our systems of interest, namely cellular and sub-cellular scale biomembrane dynamics, we should not neglect the influence of thermal fluctuations. We model the interaction of our membrane with a thermal reservoir through the addition of a stochastic fluctuating force on the membrane. That is, we now have

$$\mathcal{F}(\mathbf{r},t) = -\frac{\delta E}{\delta h}(\mathbf{r},t) + \xi(\mathbf{r},t),$$

where $\xi(\mathbf{r},t)$ is the random force satisfying the appropriate *fluctuation-dissipation theorem.* It turns out that, once again, things are easier in Fourier space. As we worked out above, $\dot{h}_{\mathbf{k}} = \Lambda_{\mathbf{k}}\mathcal{F}_{\mathbf{k}}$. With our stochastic force this is now

$$\dot{h}_{\mathbf{k}}(t) = -\Lambda_{\mathbf{k}}(\kappa k^4 + \sigma k^2)h_{\mathbf{k}}(t) + \Lambda_{\mathbf{k}}\xi_{\mathbf{k}}(t).$$

We can construct the solution for a time-dependent source, such as our noise term $\Lambda_{\mathbf{k}}\xi_{\mathbf{k}}(t)$, via convolution with the Green's function eqn. (25):

$$h_{\mathbf{k}}(t) = \int_{-\infty}^{\infty} \mathrm{d}t' h_{\mathbf{k}}^{\mathrm{GF}}(t')\Lambda_{\mathbf{k}}\xi_{\mathbf{k}}(t-t') = \int_{0}^{\infty} \mathrm{d}t' e^{-\Lambda_{\mathbf{k}}(\kappa k^4+\sigma k^2)t'}\Lambda_{\mathbf{k}}\xi_{\mathbf{k}}(t-t'). \tag{27}$$

Our strategy now is to calculate the power spectrum $\langle|h_{\mathbf{k}}|^2\rangle$ according to this solution and then compare it with the result of the equipartition theorem. We will assume the following properties for our noise ξ,

$$\langle\xi_{\mathbf{k}}(t)\rangle = 0, \tag{28}$$
$$\langle\xi_{\mathbf{k}_1}(t_1)\xi^*_{\mathbf{k}_2}(t_2)\rangle = C(\mathbf{k})\delta_{\mathbf{k}_1,\mathbf{k}_2}\delta(t_1-t_2), \tag{29}$$

where $C(\mathbf{k})$ is an as yet unknown function. The Kronecker delta is there because the modes propagate independently in Fourier space and thus have independent noise, and the Dirac delta means that the fluctuations are so-called *white noise.* Strictly speaking, this last part is not essential, but the time correlation should decay much faster than the timescale of the deterministic dynamics in order for the following calculations to remain approximately valid. The undulation power spectrum is then

$$\begin{aligned}
\langle|h_{\mathbf{k}}|^2\rangle = \langle h_{\mathbf{k}}(t)h^*_{\mathbf{k}}(t)\rangle &= \left\langle \int_0^\infty \mathrm{d}t_1 e^{-\Lambda_{\mathbf{k}}(\kappa k^4+\sigma k^2)t_1}\Lambda_{\mathbf{k}}\xi_{\mathbf{k}}(t-t_1)\int_0^\infty \mathrm{d}t_2 e^{-\Lambda_{\mathbf{k}}(\kappa k^4+\sigma k^2)t_2}\Lambda_{\mathbf{k}}\xi^*_{\mathbf{k}}(t-t_2)\right\rangle \\
&= \int_0^\infty \mathrm{d}t_1 \int_0^\infty \mathrm{d}t_2\, e^{-\Lambda_{\mathbf{k}}(\kappa k^4+\sigma k^2)(t_1+t_2)}\Lambda_{\mathbf{k}}^2 \langle\xi_{\mathbf{k}}(t-t_1)\xi^*_{\mathbf{k}}(t-t_2)\rangle \\
&= \int_0^\infty \mathrm{d}t_1 \int_0^\infty \mathrm{d}t_2\, e^{-\Lambda_{\mathbf{k}}(\kappa k^4+\sigma k^2)(t_1+t_2)}\Lambda_{\mathbf{k}}^2 C(\mathbf{k})\delta(t_2-t_1) \\
&= C(\mathbf{k})\Lambda_{\mathbf{k}}^2 \int_0^\infty \mathrm{d}t_1\, e^{-\Lambda_{\mathbf{k}}(\kappa k^4+\sigma k^2)2t_1} \\
&= C(\mathbf{k})\Lambda_{\mathbf{k}}^2 \left(\frac{1}{2\Lambda_{\mathbf{k}}(\kappa k^4+\sigma k^2)}\right) \\
\langle|h_{\mathbf{k}}|^2\rangle &= \frac{C(\mathbf{k})\Lambda_{\mathbf{k}}}{2(\kappa k^4+\sigma k^2)}.
\end{aligned} \tag{30}$$

This is the first half of what we need. Next, we write the small gradient Helfrich energy eqn. (18) for the principal $[0,L]\times[0,L]$ patch (so that the energy is finite) in our Fourier basis with the help of the derivatives we computed before,

$$E = \int_{[0,L]^2} \mathrm{d}x\mathrm{d}y \left\{ \frac{1}{2}\kappa\left(-\frac{1}{L}\sum_{\mathbf{k}} k^2 h_{\mathbf{k}} e^{i\mathbf{k}\cdot\mathbf{r}}\right)^2 + \frac{1}{2}\sigma\left(\frac{1}{L}\sum_{\mathbf{k}} i h_{\mathbf{k}}\mathbf{k} e^{i\mathbf{k}\cdot\mathbf{r}}\right)^2 \right\}$$

$$
\begin{aligned}
&= \frac{1}{L^2} \int\limits_{[0,L]^2} \mathrm{d}x\mathrm{d}y \left\{ \frac{1}{2}\kappa \sum_{\mathbf{k},\mathbf{k}'} k^2 k'^2 h_{\mathbf{k}} h_{\mathbf{k}'} e^{i(\mathbf{k}+\mathbf{k}')\cdot\mathbf{r}} - \frac{1}{2}\sigma \sum_{\mathbf{k},\mathbf{k}'} h_{\mathbf{k}} h_{\mathbf{k}'} \mathbf{k}\cdot\mathbf{k}' e^{i(\mathbf{k}+\mathbf{k}')\cdot\mathbf{r}} \right\} \\
&= \frac{1}{L^2} \int\limits_{[0,L]^2} \mathrm{d}x\mathrm{d}y \sum_{\mathbf{k},\mathbf{k}'} \left(\frac{1}{2}\kappa k^2 k'^2 - \frac{1}{2}\sigma \mathbf{k}\cdot\mathbf{k}' \right) h_{\mathbf{k}} h_{\mathbf{k}'} e^{i(\mathbf{k}+\mathbf{k}')\cdot\mathbf{r}} \\
&= \sum_{\mathbf{k},\mathbf{k}'} \left(\frac{1}{2}\kappa k^2 k'^2 - \frac{1}{2}\sigma \mathbf{k}\cdot\mathbf{k}' \right) h_{\mathbf{k}} h_{\mathbf{k}'} \frac{1}{L^2} \int\limits_{[0,L]^2} \mathrm{d}x\mathrm{d}y\, e^{i(\mathbf{k}+\mathbf{k}')\cdot\mathbf{r}} \\
&= \sum_{\mathbf{k},\mathbf{k}'} \left(\frac{1}{2}\kappa k^2 k'^2 - \frac{1}{2}\sigma \mathbf{k}\cdot\mathbf{k}' \right) h_{\mathbf{k}} h_{\mathbf{k}'} \delta_{\mathbf{k}',-\mathbf{k}} \\
&= \sum_{\mathbf{k}} \left(\frac{1}{2}\kappa k^4 + \frac{1}{2}\sigma k^2 \right) h_{\mathbf{k}} h_{-\mathbf{k}} \\
&= \sum_{\mathbf{k}} \left(\frac{1}{2}\kappa k^4 + \frac{1}{2}\sigma k^2 \right) |h_{\mathbf{k}}|^2,
\end{aligned}
$$

wherein the last line we used $h_{-\mathbf{k}} = h^*_{\mathbf{k}}$, which follows from requiring $h(\mathbf{r}, t) \in \mathbb{R}$. The equipartition theorem then immediately yields the famous membrane undulation spectrum,

$$
\left\langle \left(\frac{1}{2}\kappa k^4 + \frac{1}{2}\sigma k^2 \right) |h_{\mathbf{k}}|^2 \right\rangle = \frac{1}{2} k_{\mathrm{B}} T \quad \Longrightarrow \quad \langle |h_{\mathbf{k}}|^2 \rangle = \frac{k_{\mathrm{B}} T}{\kappa k^4 + \sigma k^2}. \tag{31}
$$

Equating this with our result above, we have

$$
\frac{C(\mathbf{k})\Lambda_{\mathbf{k}}}{2(\kappa k^4 + \sigma k^2)} = \frac{k_{\mathrm{B}} T}{\kappa k^4 + \sigma k^2} \quad \Longrightarrow \quad C(k) = 2\Lambda_{\mathbf{k}}^{-1} k_{\mathrm{B}} T = 8\eta k\, k_{\mathrm{B}} T. \tag{32}
$$

This is the fluctuation-dissipation relation we need. It relates the variance of the equilibrium thermal fluctuations, $C(k)$, to the dissipation arising from the fluid viscosity η. From this we get the power spectrum for our fluctuating force:

$$
\boxed{\langle \xi_{\mathbf{k}}(t_1) \xi^*_{\mathbf{k}}(t_2) \rangle = \frac{2k_{\mathrm{B}} T}{\Lambda_{\mathbf{k}}} \delta(t_1 - t_2) = 8\eta k\, k_{\mathrm{B}} T\, \delta(t_1 - t_2)} \tag{33}
$$

3 Numerical Simulation

3.1 Finite Timestep Noise

The transformation of the equation of motion eqn. (23) into a finite-timestep numerical algorithm is straightforward, save for the noise term. That is, we need to turn our fluctuation power spectrum eqn. (33) into a random displacement in a finite interval Δt. Let us start by integrating the fluctuation term over this interval,[3]

$$
R_{\mathbf{k}}(\Delta t) \equiv \int\limits_0^{\Delta t} \Lambda_{\mathbf{k}} \xi_{\mathbf{k}} \mathrm{d}t.
$$

Since $\langle \xi_{\mathbf{k}} \rangle = 0$, the variance of this term is just

$$
\langle |R_{\mathbf{k}}|^2 \rangle = \Lambda^2_{\mathbf{k}} \int\limits_0^{\Delta t} \mathrm{d}t_1 \int\limits_0^{\Delta t} \mathrm{d}t_2 \langle \xi^*_{\mathbf{k}}(t_1) \xi_{\mathbf{k}}(t_2) \rangle = 2k_{\mathrm{B}} T \Lambda_{\mathbf{k}} \int\limits_0^{\Delta t} \mathrm{d}t_1 \int\limits_0^{\Delta t} \mathrm{d}t_2 \delta(t_1 - t_2) = 2k_{\mathrm{B}} T \Lambda_{\mathbf{k}} \Delta t. \tag{34}
$$

But, we must keep in mind that $R_{\mathbf{k}}$ is complex-valued, so $R_{\mathbf{k}} = a_{\mathbf{k}} + ib_{\mathbf{k}}$, with a and b real. These are each taken to be i.i.d. random variables with variance $k_{\mathrm{B}} T \Lambda_{\mathbf{k}} \Delta t$ (except for pure real modes, see below), such that their sum gives the total variance $\langle |a_{\mathbf{k}} + ib_{\mathbf{k}}|^2 \rangle = \langle a^2_{\mathbf{k}} \rangle + \langle b^2_{\mathbf{k}} \rangle = 2k_{\mathrm{B}} T \Lambda_{\mathbf{k}} \Delta t$ as above. Assuming that this random displacement is due to a constant barrage of particles in the surrounding medium, and given the finite variance of the displacement distribution, we may conclude by the Central Limit Theorem that these random variables should be Gaussian, and thus are now fully specified.

[3]Since the prefactor of the fluctuation does not depend on the current value of the random walk $h_{\mathbf{k}}$, we need not worry about Itô *vs.* Stratonovich integration here; they yield the same result.

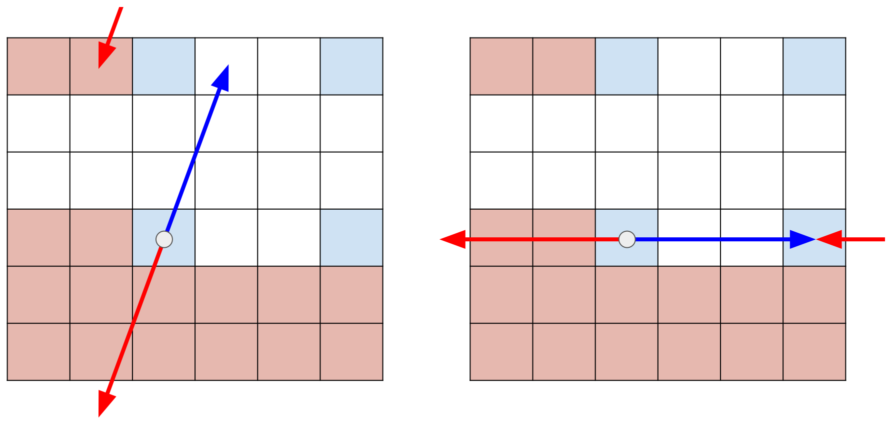

Figure 2: Diagram of independent complex and pure real modes. Each square represents one of the N^2 (depicted here for $N = 6$) Fourier modes corresponding to a particular $\mathbf{k}$ vector. The grey circle indicates the zero mode $\mathbf{k} = 0$. White squares are modes chosen to be independent complex degrees of freedom (2 real degrees of freedom). Red squares indicate modes which are fully determined by the corresponding $-\mathbf{k}$ mode, due to the condition that $h_{-\mathbf{k}} = h^*_{\mathbf{k}}$. Blue modes are pure real degrees of freedom due to $-\mathbf{k}$ coinciding with $\mathbf{k}$ in the first Brillouin zone (as exemplified in the diagram on the right). Adding up the number of independent real degrees of freedom in Fourier space then gives $4 + (2 \times 16) = 36 = N^2$, exactly matching the real-space representation.

3.2 Mode Counting

We will work with a computer implementation where we keep track of the real-space positions $h(x, y) \in \mathbb{R}$ subject to periodic boundary conditions on a discrete square lattice with spacing $a = L/N$ (that is, $x_n = na/L$, $n = 0, 1, \ldots, N - 1$, and the same for y). We then evidently have, in total, N^2 real degrees of freedom that can vary in our simulation. Our Fourier series representation of h in eqn. (22) sums over $\mathbf{k} = \frac{2\pi}{L}(n\hat{\mathbf{x}} + m\hat{\mathbf{y}})$. To guarantee that h is real in this representation, we sum over both positive and negative values of n and m (the imaginary part of $h_{-\mathbf{k}}$ cancels that of $h_{\mathbf{k}}$). The existence of our discrete lattice length a means that we have an upper bound on $\mathbf{k}$-vector components. This also means that components larger than π/a “wrap back around” to the other half of the first Brillouin zone.

The combination of the condition of realness and the periodicity of $\mathbf{k}$-space gives rise to some odd subtleties in how simulations must be propagated. Fig. 2 shows a diagram of independent real and complex modes in our discrete, finite $\mathbf{k}$-space. Independent thermal noise should only be applied to $h_{\mathbf{k}}$ variables which are independent, with the dependent $h_{-\mathbf{k}}$ modes being assigned the complex conjugate value. Pure real modes (blue in Fig. 2) must still satisfy eqn. (34), meaning the noise term must have twice the variance of the constituent real components of a complex mode. An unfortunate fact is that the independent/dependent mode bookkeeping is simpler for odd N, but discrete FFT codes are universally more efficient for even N.

References

[1] F Brochard and JF Lennon. “Frequency spectrum of the flicker phenomenon in erythrocytes”. In: *Journal de Physique* 36.11 (1975), pp. 1035–1047.

[2] Markus Deserno. “Fluid lipid membranes: From differential geometry to curvature stresses”. In: *Chemistry and Physics of Lipids* 185 (2015), pp. 11–45.

[3] Masao Doi and Samuel Frederick Edwards. *The Theory of Polymer Dynamics*. Vol. 73. Oxford University Press, 1988.

[4] Lawrence C-L Lin and Frank LH Brown. “Brownian dynamics in Fourier space: membrane simulations over long length and time scales”. In: *Physical Review Letters* 93.25 (2004), p. 256001.

[5] Udo Seifert. “Configurations of fluid membranes and vesicles”. In: *Advances in physics* 46.1 (1997), pp. 13–137.

[6] Eric W Weisstein. “Bessel Function of the First Kind”. In: *MathWorld–A Wolfram Web Resource* (2024). URL: `https://mathworld.wolfram.com/BesselFunctionoftheFirstKind.html`.